REPORT DOCUMENTATION PAGE

Form Approved OMB NO. 0704-0188

1. REPORT DATE (DD-MM-YYYY)	2. REPORT TYPE	3. DATES COVERED (From - To)
	New Reprint	-

4. TITLE AND SUBTITLE

Surfactant assisted synthesis of aluminum doped SrFe10Al2O19 hexagonal ferrite

5a. CONTRACT NUMBER
W911NF-11-1-0507
5b. GRANT NUMBER
5c. PROGRAM ELEMENT NUMBER
611102
5d. PROJECT NUMBER
5e. TASK NUMBER
5f. WORK UNIT NUMBER

6. AUTHORS

D. Neupane, L. Wang, S. R. Mishra, N. Poudyal, J. P. Liu

7. PERFORMING ORGANIZATION NAMES AND ADDRESSES

University of Texas at Arlington
701 S. Nedderman Drive
Box 19145
Arlington, TX 76019 -0145

8. PERFORMING ORGANIZATION REPORT NUMBER

9. SPONSORING/MONITORING AGENCY NAME(S) AND ADDRESS (ES)

U.S. Army Research Office
P.O. Box 12211
Research Triangle Park, NC 27709-2211

10. SPONSOR/MONITOR'S ACRONYM(S)
ARO

11. SPONSOR/MONITOR'S REPORT NUMBER(S)
60580-MS.16

12. DISTRIBUTION AVAILIBILITY STATEMENT

Approved for public release; distribution is unlimited.

13. SUPPLEMENTARY NOTES

The views, opinions and/or findings contained in this report are those of the author(s) and should not contrued as an official Department of the Army position, policy or decision, unless so designated by other documentation.

14. ABSTRACT

M-type aluminum doped SrFe10Al2O19 were synthesized via co-precipitation method using cetyltrimethyl ammonium bromide (CTAB) as a surfactant. The effects of CTAB content (x¼0, 1, 3, and 9wt. %) on the formation, structure, morphology, magnetic, and dielectric properties of the SrFe10Al2O19 nanoparticles were investigated. X-ray diffraction results show elimination of a-Fe2O3 phase from samples prepared using CTAB. Morphological changes including grain and crystallite size was noticed with the increase in the CTAB content. With the increase in CTAB, powder particles grew

15. SUBJECT TERMS

surfactants, ferrite magnets

16. SECURITY CLASSIFICATION OF:			17. LIMITATION OF ABSTRACT	15. NUMBER OF PAGES	19a. NAME OF RESPONSIBLE PERSON
a. REPORT	b. ABSTRACT	c. THIS PAGE			Ping Liu
UU	UU	UU	UU		19b. TELEPHONE NUMBER 817-272-2815

Report Title

Surfactant assisted synthesis of aluminum doped SrFe10Al2O19 hexagonal ferrite

ABSTRACT

M-type aluminum doped SrFe10Al2O19 were synthesized via co-precipitation method using cetyltrimethyl ammonium bromide (CTAB) as a surfactant. The effects of CTAB content (x¼0, 1, 3, and 9wt. %) on the formation, structure, morphology, magnetic, and dielectric properties of the SrFe10Al2O19 nanoparticles were investigated. X-ray diffraction results show elimination of a-Fe2O3 phase from samples prepared using CTAB. Morphological changes including grain and crystallite size was noticed with the increase in the CTAB content. With the increase in CTAB, powder particles grew in hexagonal plates. A linear increase in saturation magnetization, Ms, with CTAB content was observed from 56.5 emu/g at 0% CTAB to 66.4 emu/g at 9% CTAB. This is a net increase of 17.5% in Ms. The coercivity (Hc┐5700 Oe) of sample reached maximum at 1% CTAB and reduced with further CTAB content reaching to a minimum value of 4488 Oe at 9% CTAB. A slight increase in Curie temperature (735 K) was also observed for samples synthesized using CTAB as compared to that of sample prepared in the absence of CTAB (729 K). Samples synthesized with CTAB show higher dielectric constants as compared to samples prepared without CTAB, while dielectric constant for all samples show decrease in value with the increase in frequency. These results imply that CTAB may act as a crystallization master, controlling the nucleation and growth of SrFe10Al2O19 crystal. The study delineates the scope of improving magnetic properties of ferrites without substitution of metal ions.

REPORT DOCUMENTATION PAGE (SF298)
(Continuation Sheet)

Continuation for Block 13

ARO Report Number 60580.16-MS
Surfactant assisted synthesis of aluminum dope...

Block 13: Supplementary Note

Approved for public release; distribution is unlimited.

AIP Journal of Applied Physics

Surfactant assisted synthesis of aluminum doped SrFe10Al2O19 hexagonal ferrite

D. Neupane, L. Wang, S. R. Mishra, N. Poudyal, and J. P. Liu

Citation: Journal of Applied Physics **117**, 17D158 (2015); doi: 10.1063/1.4919254
View online: http://dx.doi.org/10.1063/1.4919254
View Table of Contents: http://scitation.aip.org/content/aip/journal/jap/117/17?ver=pdfcov
Published by the AIP Publishing

Surfactant assisted synthesis of aluminum doped $SrFe_{10}Al_2O_{19}$ hexagonal ferrite

D. Neupane,[1,a)] L. Wang,[1] S. R. Mishra,[1] N. Poudyal,[2] and J. P. Liu[2]
[1]*Department of Physics, The University of Memphis, Memphis, Tennessee 38152, USA*
[2]*Department of Physics, The University of Texas, Arlington, Texas 76019, USA*

(Presented 4 November 2014; received 22 September 2014; accepted 23 January 2015; published online 5 May 2015)

M-type aluminum doped $SrFe_{10}Al_2O_{19}$ were synthesized via co-precipitation method using cetyltrimethyl ammonium bromide (CTAB) as a surfactant. The effects of CTAB content (x = 0, 1, 3, and 9 wt. %) on the formation, structure, morphology, magnetic, and dielectric properties of the $SrFe_{10}Al_2O_{19}$ nanoparticles were investigated. X-ray diffraction results show elimination of α-Fe_2O_3 phase from samples prepared using CTAB. Morphological changes including grain and crystallite size was noticed with the increase in the CTAB content. With the increase in CTAB, powder particles grew in hexagonal plates. A linear increase in saturation magnetization, Ms, with CTAB content was observed from 56.5 emu/g at 0% CTAB to 66.4 emu/g at 9% CTAB. This is a net increase of 17.5% in Ms. The coercivity (Hc ~ 5700 Oe) of sample reached maximum at 1% CTAB and reduced with further CTAB content reaching to a minimum value of 4488 Oe at 9% CTAB. A slight increase in Curie temperature (735 K) was also observed for samples synthesized using CTAB as compared to that of sample prepared in the absence of CTAB (729 K). Samples synthesized with CTAB show higher dielectric constants as compared to samples prepared without CTAB, while dielectric constant for all samples show decrease in value with the increase in frequency. These results imply that CTAB may act as a crystallization master, controlling the nucleation and growth of $SrFe_{10}Al_2O_{19}$ crystal. The study delineates the scope of improving magnetic properties of ferrites without substitution of metal ions. [http://dx.doi.org/10.1063/1.4919254]

Among ferrites family, M-type hexagonal ferrites finds host of applications ranging from simple permanent magnets microwave applications. In a push to improve magnetization and microwave properties of M-type ferrite, various strategies including shape and size, grain refinement, and anisotropy changes are employed via substitutional atoms, magnetic or non-magnetic, for either Fe^{3+} or Sr^{2+}.[1–5]

It was recently reported that Al^{3+} substitution brings in large 300% increase in coercivity.[6,7] However, a concomitant reduction in magnetization was evident due to replacement of magnetic Fe^{3+} with non-magnetic Al^{3+}. The reduction in magnetization was also attributed to the grain refinement, lattice, and surface defects, which decreases the net magnetic moment per unit volume. Decrease in coercivity is also often reported in ferrites either resulting from grain refinement or presence of secondary phase α-Fe_2O_3 in the sample. In order for Sr-ferrite to be useful for permanent magnet applications, it is necessary that high magnetization along with high coercivity values be maintained.

Recently, cetyltrimethyl ammonium bromide (CTAB) has been used in the synthesis of ferrites, such as $CoFe_2O_4$, $BaFe_{12}O_{19}$, and $SrFe_{12}O_{19}$, as a cationic surfactant.[8–10] Cationic surfactant, CTAB, has generally been used as templating micelle molecule to synthesize mesoporous materials[11–13] to control the morphology and oriented growth of metal-oxide nanocrystals. Particularly, in ferrites, it is reported that CTAB assisted growth can eliminate extra magnetic phase and modify nanostructural morphology which can concomitantly improve the magnetization and coercivity.[10,14]

In view of this, CTAB assisted growth of $Sr_2Fe_{10}Al_2O_{19}$ is studied with an expectation for improving magnetization, coercivity, and dielectric properties of the same. Importantly, the study delineates the scope of improving magnetic properties of M-type hexagonal ferrites without substitution of metal ions, a fact that can reduce the production of cost ferrites.

M-type Al^{3+} doped strontium ferrite $SrFe_{10}Al_2O_{19}$ samples were prepared via wet chemical method. Stoichiometric amount of analytical grade $Fe(NO_3)_3{\cdot}9H_2O$ (4.02435 g), $Sr(NO_3)_2$ (0.21081 g), and $Al(NO_3)_3{\cdot}9H_2O$ (0.74735 g) in water solution (Fe^{3+}/Sr^{2+} mole ratio = 11) was dropped into a NaOH (4 g in 250 ml of water) solution and stirred at 400 rpm for 20 min. CTAB was added as a surfactant and the CTAB content (x = 0, 1 (0.4983 g), 3 (0.14948 g), 6 (0.29895 g), and 9 (0.44843 g) wt. %) was varied according to the weight of nitrate salts. The obtained precipitates were filtered, washed, and then dried in an oven at 70 °C for 10 h, followed by heat treatment at 900 °C for 10 h in air to get the hexaferrite phase.

The crystal structures of the samples were identified by x-ray diffraction (XRD, Bruker D8 diffractometer) with Cu K_α radiation. Field emission scanning electronic microscopy (FESEM, FEI) was used to investigate the particle size and morphology of $SrFe_{10}Al_2O_{19}$ powder particle. Saturation magnetization (Ms) and intrinsic coercivity (Hc) were measured at room temperature (RT) using a vibrating sample magnetometer (VSM). Curie temperature, Tc, was measured

a)Author to whom correspondence should be addressed. Electronic mail: dneupane@memphis.edu.

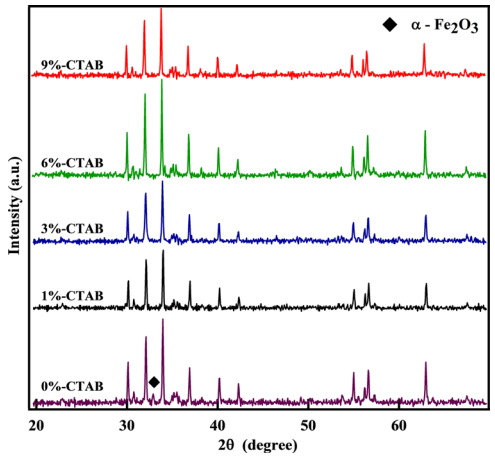

FIG. 1. XRD patterns of $SrFe_{10}Al_2O_{19}$ samples prepared with different amount of CTAB.

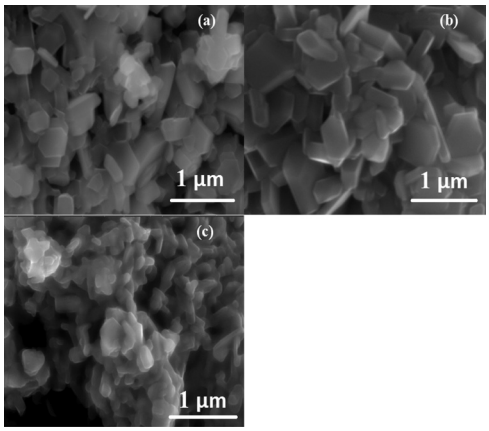

FIG. 2. SEM images of $SrFe_{10}Al_2O_{19}$ prepared using (a) 0%, (b) 6%, and (c) 9% CTAB. Scale bar is 1 μm.

using thermogravimetric analysis (TGA) under magnetic field. Dielectric properties were measured using 4275A Multi-Frequency LCR meter. Dielectric measurements were made on 1 cm diameter disc samples prepared at 6 MPa and annealed at 600 °C for 10 h.

XRD patterns of as-synthesized samples are shown in Fig. 1. It is evident from Fig. 1 that CTAB assisted synthesis lead to the formation of single phase $SrFe_{10}Al_2O_{19}$ powder. Powder prepared without CTAB show the presence of α-Fe_2O_3. Clearly benefit of using CTAB in eliminating α-Fe_2O_3 phase from the ferrite powder is evident. Lattice parameters, *a*, *c*, and *V*, were calculated via profile fitting of XRD patterns using TOPAS software. An increase in lattice volume is observed for samples prepared using CTAB (Table I). This increase in lattice volume again corroborate the fact that Fe^{3+} which were phase separated in Fe_2O_3 in samples prepared without CTAB are now well dissolved in samples prepared with CTAB assistance.

SEM images of CTAB assisted growth of $SrFe_{10}Al_2O_{19}$ is shown in Fig. 2. The sample prepared without CTAB shows hexagonal plates and rods (0% CTAB). However, samples prepared with CTAB show grain growth. For example, 6% CTAB sample show the presence of ultrathin hexagonal plates of size around 650 nm. The plate like growth of particles continues up to 6% CTAB but at higher CTAB content, growth of small agglomerated particles is evident. Although hexagonal platelet-like $SrFe_{12}O_{19}$ particles have been obtained by various methods without CTAB addition,[10,15,16] high heat treatment or long temperature-holding time were necessary, giving rise to large particle size (>1 μm). Herein, sub-micron size hexagonal platelets are prepared at relatively low temperature with the help of cationic CTAB surfactant. When the molecule of CTAB is present in the reacting medium, it hydrolyzes and its ions are electrostatically attracted by the negatively charged hydroxides of Fe, Sr, and Al. By surrounding them, CTAB molecules act like a barrier hindering some reactions of taking place.[17–20] Furthermore, the CTAB prevents the transformation of $Fe(OH)_6^{3-}$ into FeO(OH), a contaminant leading to the formation of α-Fe_2O_3.

TABLE I. Crystallite size and microdeformation parameters of $SrFe_{10}Al_2O_{19}$ as a function of CTAB content obtained from HWL plot.

CTAB content (%)	a (Å)	c (Å)	V (Å)^3	Crystallite size (nm)	ε (-)
0	5.8709	23.0097	686.83	66.22 ± 0.02	0.002
1	5.8818	23.0609	690.92	66.66 ± 0.02	0.224
3	5.8688	23.0113	686.38	68.49 ± 0.02	0.002
6	5.8746	23.0277	688.24	68.02 ± 0.02	0.003
9	5.8836	23.0376	690.64	65.36 ± 0.02	0.002

The presence of two distinct morphologies, namely, rods and hexagonal plates, has been explained on the basis of presence of Fe_2O_3 in sample.[10] The presence of Fe_2O_3 provides rough interface between spherical $SrFeO_{3-x}$ and Fe_2O_3 precursors leading to the growth of rod like particles. In the presence of CTAB, owing to selective adsorption of CTAB to a certain crystal plane, the smooth reaction interface leads to the formation of hexagonal platelet-like particles. The growth rate is relatively low along the {001} direction but relatively high in {hk0} direction.[10] Consequently, ultrathin hexagonal platelets of hexaferrites have been obtained.

The mean crystallite size was deduced from the Halder-Wagner-Langford's (HWL) plot technique[21] applied to the XRD data. The HWL equation relates the FWHM of peaks, β, with the mean crystallize size, "T," and the microdeformation of a grain, ε as follows:

$$\left(\frac{\beta^*}{d^*}\right)^2 = \frac{1}{T}\left(\frac{\beta^*}{d^{*2}}\right) + \left(\frac{\varepsilon}{2}\right),$$

where β^* is given by $\beta^* = \frac{\beta}{\lambda}\cos(\theta)$, where λ is the x-rays wavelength and d* is given as $d^* = \frac{2}{\lambda}\sin(\theta)$.

Figure 3 presents the HWL plots for the samples. Crystallite size and microstrain derived from the plot is shown in Table I.

From Table I, it is evident that CTAB brings in certain degree of crystallite growth along with some microdeformation. This is in agreement with the previous studies on the influence of surfactant on the microdeformation of nanopowders.[22] A decrease in crystallite size is noticed in 9% CTAB sample. This fact is also corroborated by the SEM images, Fig. 2, showing smaller grains for the same.

Figure 4 shows the RT M-H demagnetization curves of $SeFe_{10}Al_2O_{19}$ powders prepared with different CTAB contents. The RT magnetic parameters extracted from the demagnetization loops are tabulated in Table II. The variation in Ms

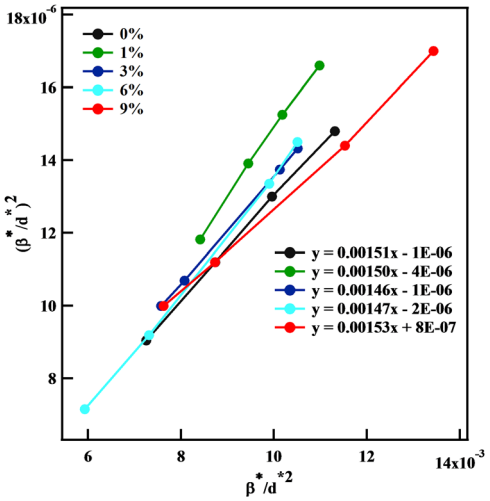

FIG. 3. HWL plots for $SrFe_{10}Al_2O_{19}$ as a function of CTAB content obtained from XRD.

and Hc with CTAB content is shown in Fig. 5. The optimal value Ms was 66.41 emu/g at 9% CTAB content. Compared with the Ms value of samples prepared in the absence of CTAB (56.54 emu/g), a maximum improvement with CTAB in Ms of 17.46% is observed. With the addition of CTAB surfactant, single phase highly crystalline $SrFe_{12}O_{19}$ was obtained, leading to the remarkable enhancement in *Ms*.

CTAB assisted samples, a maximum in coercivity (~5667 Oe) was observed for 1%–3% CTAB samples. A net gain in coercivity is about 5% at 1% CTAB as compared to that of sample prepared without CTAB. The elimination of extra phase, α-Fe_2O_3, in CTAB samples may also contribute to the coercivity enhancement. However, the coercivity declined with the increase in CTAB content above three percent. The decrease in coercivity is obvious with the increase in the grain size of multidomain particles. The formation of multi-domain and the easy movement of the domain walls result in the decrease of coercivity. The critical size domain calculation for as synthesized ferrite particles is discussed below.

All samples prepared using CTAB show higher Tc (Tc ~ 735 K) value in comparison to the one prepared without CTAB assistance (Tc ~ 729 K). The observed increase in Tc may be attributed to the enhanced Fe^{3+}-O^{2-}-Fe^{3+} superexchange resulting from volume expansion and increase in

TABLE II. Room temperature magnetic parameters of $SrFe_{10}Al_2O_{19}$ prepared using CTAB.

CTAB (%)	Ms (emu/g)	Mr (emu/g)	Mr/Ms	Hc (Oe)	Ms (G)	Tc (K)	Dm (nm)
0	56.5	27.8	0.49	5352.3	288	729	613
1	58.1	30.1	0.51	5667.0	296	735	615
3	61.3	30.6	0.49	5604.2	312	735	616
6	61.7	30.1	0.48	4268.1	314	735	616
9	66.4	32.8	0.49	4488.2	338	735	615

magnetization. The values of squareness ratio (M_r/M_s) for all samples are in the range of ~0.5, which indicates the particles are most likely non-interacting single domain particles.[23,24] In this case, the magnetization mainly depends on the magnetic domain rotation, so the coercivity can be calculated by Stoner-Wohlfarth theory, $H_c = 2\,K/(\mu_0 M_s)$, where K is magnetocrystalline anisotropy constant and μ_0 is vacuum permeability. It clear that Hc has inverse dependence on Ms. This implies higher Ms leads to low Hc values.

Having size dependence, coercivity can also be analyzed in view of the size variation in nanoparticles. When the size of a ferro- or ferri-magnetic particle decreases to a certain critical value, the particles change from a state with multiple magnetic domains to one with a single domain. When the particle size is much larger than the critical size of a single domain, the coercivity is determined by magnetic displacement of domain walls, so the value of coercive force is small. When the particle size is reduced to the critical size of single domain, the coercivity is determined by magnetic domain rotation, so the coercivity reaches the maximum. When the particle size is less than the critical size of a single domain, the coercivity will decrease for the existence of superparamagnetism. The average grain size of the $SrFe_{10}Al_2O_{19}$ particles prepared using 0%, 6%, and 9% CTAB is 300 nm, 650 nm, and 150 nm. The critical size of a single-domain particle is estimated using the following equation:[15,25]

$$D_m = 9\sigma_W/(2\pi M_s^2), \quad (1)$$

where $\sigma_W = (2k_B T_C|K|/a)^{1/2}$ is the wall density energy, $|K|$ is the magnetocrystalline anisotropy constant, T_C is the Curie temperature, M_S is the saturation magnetization, k_B is the Boltzmann

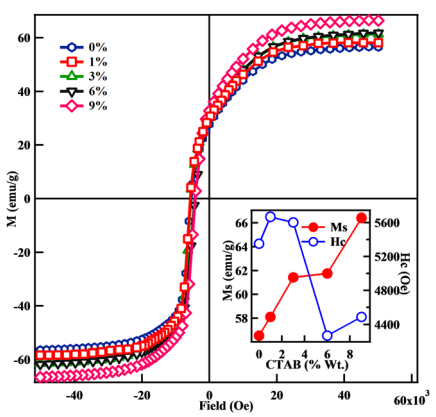

FIG. 4. Room temperature demagnetization curves of $SrFe_{10}Al_2O_{19}$ as a function of CTAB content.

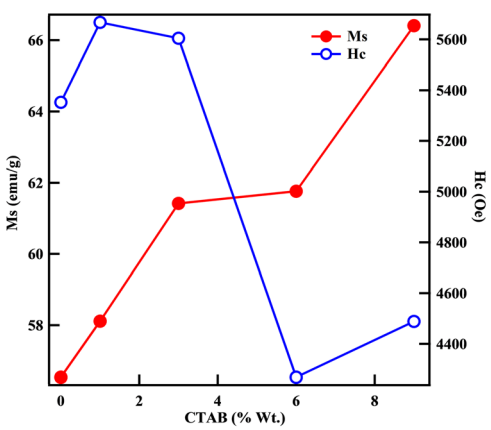

FIG. 5. Magnetic parameters, Ms and Hc, as extracted from demagnetization curves for $SrFe_{10}Al_2O_{19}$ as a function of CTAB content.

constant, and a is the lattice constant. For *grain size (D)* $> D_m$, the particles are multi-domain structures, while for $D < D_m$, the particles are mono-domain structures. Table I lists D_m values calculated using Eq. (1). For $SrFe_{10}Al_2O_{19}$ prepared without CTAB, $T_C = 729\,K$, $a = 5.8709 \times 10^{-6}$ cm, assuming $|K| = 3.7 \times 10^6$ erg/cm^3 for $SrFe_{12}O_{19}$,[26] and $M_s = 288$ gauss, the estimated value of D_m is about 613 nm, while for $SrFe_{10}A_{l2}O_{19}$ prepared with CTAB, the critical domain size value is about 616 nm. Thus, the critical domain size is greater than the observed grain size for 0% and 9% CTAB samples while smaller than critical grain size value for 6% CTAB sample. Thus, particles synthesized with CTAB content below 6% are approximated as single domain particles while particles prepared at 6% CTAB could be multidomain. This explains the observed increase in coercivity of samples prepared below and above 6% CTAB content. The formation of multi-domain and the easy movement of the domain walls result in the decrease of the coercivity as observed in 6% CTAB sample. On the other hand, in M-type strontium hexaferrite, the magnetic easy axis lies within the basal plane. The demagnetizing factor in a disk shape for a $SrFe_{10}Al_2O_{19}$ particle increases with the increase of the width to thickness ratio, which leads to a decrease in coercivity as well.[23] Consequently, as shown in Fig. 3, the regular hexagonal plate-like morphology developed for 6% CTAB samples leads to lower coercivity than the theoretical prediction.

Figure 6 represent the dielectric properties of $SrFe_{10}Al_2O_{19}$ with different CTAB contents at low frequencies. Dielectric constant (ε') decreases with increasing frequency. This behavior is normal for ferrites and is believed to be due to the interfacial polarization as predicted by Maxwell–Wagner[26] for mixtures of materials with electrically conducting regions that are not in contact with each other (separated by non-conducting regions). If the charge layers are thin and much smaller than the particle dimensions, the charge responds independently of the charge on nearby particles. At low frequencies, the charges have time to accumulate at the borders of the conducting regions causing ε' to increase. At higher frequencies, the charges do not have time to accumulate and polarization does not occur since the charge displacement is small compared to the dimensions of the conducting region. Thus, as the frequency increases, ε' decreases. The argument for the decrease in ε' with the increase in frequency is also attributed to the fact that the electron exchange between Fe^{2+} and Fe^{3+} ions cannot follow the change of the external applied field beyond certain frequency.[16] The increased crystallite size with CTAB content leads to the increase in number of domains and the volume percentage of domain wall resulting in large dielectric constant increase. With the reduction in grain/crystallite size in 9% CTAB samples, the surface charge compensation layer with a lower dielectric constant causes the total dielectric constant to decrease.

CTAB-assisted chemical co-precipitation method was adopted to synthesize $SrFe_{10}Al_2O_{19}$ particles. It is demonstrated that CTAB has a significant effect on the crystallization, morphology, grain, magnetic and dielectric properties of $SrFe_{10}Al_2O_{19}$ powders. With CTAB assistance, single phase $SrFe_{10}Al_2O_{19}$ particles ~650 nm with hexagonal platelet-like morphology were obtained. CTAB assisted samples also show the absence of α-Fe_2O_3 which otherwise is difficult to remove via any conventional synthesis methods. Magnetic properties

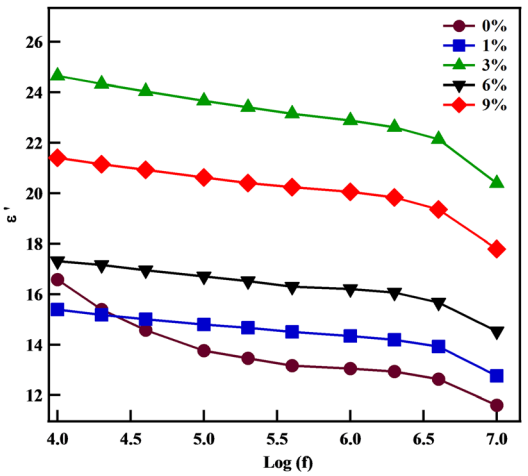

FIG. 6. Low frequency dielectric properties of $SrFe_{10}Al_2O_{19}$ as a function of CTAB content.

were remarkably improved with CTAB surfactant addition; a 17% enhancement in saturation magnetization was achieved. It is to be noted that this magnetization enhancement, in high coercivity, $SrFe_{10}Al_2O_{19}$ is highly desirable increment for permanent magnet applications. Even though the coercivity decreases at higher CTAB content, Ms and Hc values are superior to that of pure $SrFe_{12}O_{19}$ (Ms ~ 59.33 emu/g and Hc ~ 4.2 kOe) prepared via autocombustion method.[6] It is to be noted that the increase in saturation magnetization is obtained not via doping of metal ions but simply via structural modification. Thus, in conclusion, it is shown in this work that the Hc and Ms of the hexaferrite sample are closely related not only to the grain size but also to the method of preparation. It is possible to obtain high quality samples with desirable magnetic properties by optimizing the processing parameters.

The work was supported by the funds provided by NSF-CMMI (Grant No. 1029780) and NSF-TNSCORE (Grant No. EPS 1004083).

[1]L. Qiao *et al.*, J. Magn. Magn. Mater. **318**, 74 (2007).
[2]S. Ounnunkada *et al.*, J. Magn. Magn. Mater. **301**, 292 (2006).
[3]G. Albanese *et al.*, J. Magn. Magn. Mater. **15–18**, 1453 (1980).
[4]V. N. Dhage *et al.*, Physica B **406**, 789 (2011).
[5]M. R. Eraky *et al.*, Mater. Lett. **57**, 3427 (2003).
[6]H. Luo *et al.*, J. Magn. Magn. Mater. **324**, 2602 (2012).
[7]T. T. V. Nga *et al.*, J. Magn. Magn. Mater. **324**, 1141 (2012).
[8]S. L. Tang *et al.*, J. Cryst. Growth **270**, 156 (2004).
[9]Y. Du *et al.*, J. Mater. Sci. **45**, 2442 (2010).
[10]D. Y. Chen *et al.*, Mater. Lett. **76**, 84 (2012).
[11]S. Besson *et al.*, J. Phys. Chem. B **104**, 12095 (2000).
[12]D. Grosso *et al.*, J. Mater. Chem. **10**, 2085 (2000).
[13]L. Yan *et al.*, Int. J. Inorg. Mater. **3**, 633 (2001).
[14]A. L. L. Moriyamaa *et al.*, Powder Technol. **256**, 482 (2014).
[15]Z. F. Zi *et al.*, J. Magn. Magn. Mater. **320**, 2746 (2008).
[16]M. A. Rehman *et al.*, J. Alloys Compd. **509**, 435 (2011).
[17]L. Chen *et al.*, Mater. Sci. Eng. A **415**, 156 (2006).
[18]Y. X. Wang *et al.*, Ceram. Int. **37**, 3431 (2011).
[19]Q. J. He *et al.*, Microporous Mesoporous Mater. **117**, 609 (2009).
[20]L. Zhao *et al.*, J. Solid State Chem. **181**, 245 (2008).
[21]C. Halder *et al.*, J. Acta Crystallogr. **20**, 312 (1966).
[22]I. Singh *et al.*, Solid State Sci. **13**, 2011 (2011).
[23]E. C. Stoner *et al.*, Philos. Trans. R. Soc., London, Ser. A **240**, 599 (1948).
[24]A. E. Berkowitz *et al.*, *Magnetism and Metallurgy* (Academic, New York, 1969), Vol. 1, Chap. 8.
[25]A. Ataie *et al.*, J. Eur. Ceram. Soc. **21**, 1951 (2001).
[26]D. H. Choi *et al.*, IEEE Trans. Magn. **39**, 2884 (2003).